

## Morphological Behavior of Liposomes and Lipid Nanoparticles

Igor V. Zhigaltsev\* and Pieter R. Cullis

Cite This: *Langmuir* 2023, 39, 3185–3193

Read Online

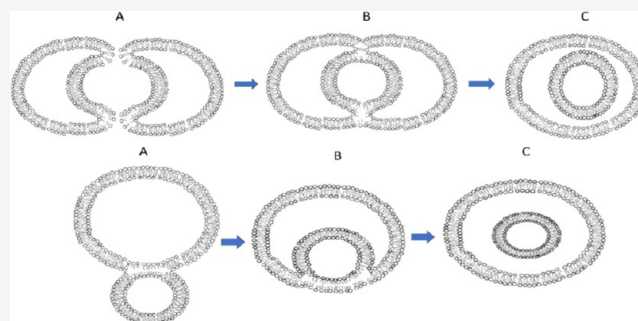
ACCESS |

Metrics &amp; More

Article Recommendations

Supporting Information

**ABSTRACT:** Liposomes, which consist of bilayer lipids surrounding interior aqueous compartment(s), were first characterized nearly 60 years ago. Remarkably, many fundamental properties of liposomes and their micellar-like “solid core” counterparts (a lipid monolayer surrounding a hydrophobic core) and transitions between these structures remain poorly understood. In this work, we examine the effects of basic variables on the morphology adopted by lipid-based systems produced by rapid mixing of lipids in ethanol with aqueous media. We show that, for lipids such as distearoylphosphatidylcholine (DSPC)–cholesterol mixtures that form bilayer vesicles on hydration, osmotic stress can induce regions of high positive membrane curvature, leading to fusion between unilamellar vesicles to produce bilamellar vesicles. Addition of lyso PC, an “inverted cone”-shaped lipid that supports regions of high positive curvature, can inhibit the formation of these bilamellar vesicles by stabilizing a hemifused intermediate structure. Conversely, the presence of “cone”-shaped lipids such as dioleoylphosphatidylethanolamine (DOPE) that results in negative membrane curvature promotes fusion events subsequent to vesicle formation (during the ethanol dialysis stage), leading to bilamellar and multilamellar systems even in the absence of osmotic stress. Alternatively, the presence of increasing amounts of triolein, a lipid that is insoluble in lipid bilayers, results in increasing internal solid core structures until micellar-like systems with a hydrophobic core of triolein are achieved. These results are interpreted in terms of the intrinsic membrane curvature that bilayer vesicles can stably maintain as well as the ability of bilayer lipids to first form a monolayer around a solid core of hydrophobic material such as triolein and then, as the proportion of bilayer lipids is increased, progressively form bilayer structures that can eventually form a complete bilayer encapsulating both a hydrophobic core and an aqueous compartment. These hybrid intermediate structures may have utility as novel drug delivery systems.



## INTRODUCTION

Liposomal systems were first described as concentric lamellae of phospholipids obtained by dispersion of lipids in water nearly 60 years ago.<sup>1</sup> Many thousands of publications since then have detailed phospholipid phase transitions,<sup>2,3</sup> methods of generating bilayer<sup>4</sup> and micellar-like<sup>5</sup> structures, as well as methods of loading liposomes with small molecules<sup>6,7</sup> and nucleic acid-based drugs.<sup>8,9</sup> This work has led to more than 12 drugs approved by the FDA and EMA that use lipid-based delivery systems, including the lipid nanoparticle (LNP) systems that enable the Covid-19 mRNA vaccines.<sup>10</sup> Despite all of these efforts, however, many basic features of aqueous dispersions of lipids remain poorly characterized. In this work, we focus on lipid dispersions formed by dilution of lipids dissolved in ethanol into an aqueous medium, a technique introduced by Batzri and Korn in 1973.<sup>11</sup> As shown in this seminal publication, this “bottom up” procedure produces very small “limit-size” vesicles that are comparable in size with the smallest size vesicles that can be produced by “top down” processes such as sonication of large multilamellar systems.<sup>12</sup> Ethanol dilution/rapid mixing processes to form lipid dispersions have become popular in recent times as they can

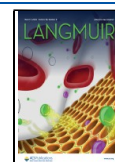
be readily applied to encapsulation of macromolecules such as nucleic acid-based drugs.<sup>13,14</sup>

Here, we investigate the basic features of lipid structures formed by ethanol dilution/rapid mixing processes using a standard method of producing these systems.<sup>14</sup> This method involves dissolving the lipids in ethanol and then mixing with an aqueous solution using a T-tube or microfluidic mixer at a 3:1 ratio (aqueous/ethanol, vol/vol) and subsequently dialyzing against phosphate-buffered saline (PBS) to remove ethanol and increase ionic strength. We ask four questions as to the morphology of the resulting lipid nanoparticles. First, what are the effects of osmotic stress on limit-size vesicles consisting of bilayer (cylindrical shape) lipids? Second, what is the effect of introducing non-bilayer (cone-shaped) lipids that contribute to a negative intrinsic radius of curvature? Third,

Received: October 13, 2022

Revised: February 14, 2023

Published: February 22, 2023



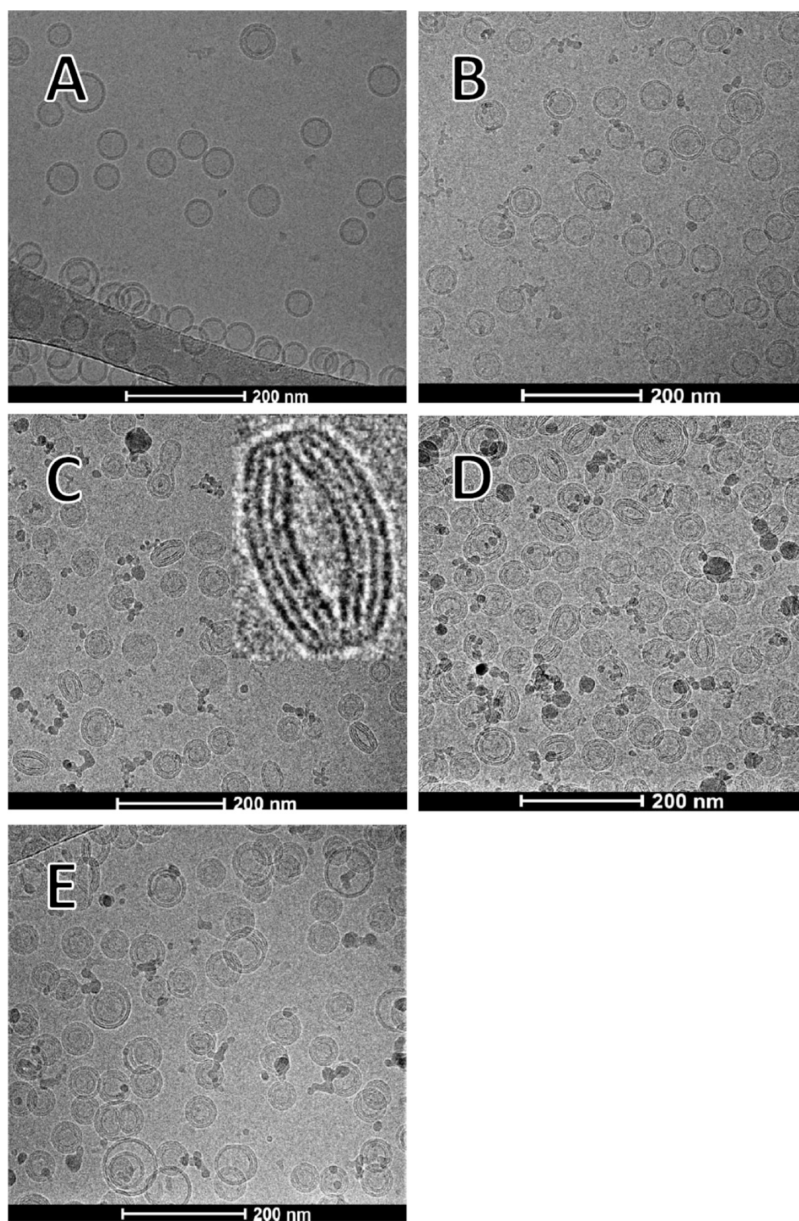


**Figure 1.** Osmotic stress can drive formation of bilamellar lipid structures for DSPC/Chol (1:1; mol/mol) vesicles as visualized by cryo-TEM. LNPs were prepared using the T-tube mixing process described in Methods. (A) LNPs were made by rapid mixing an ethanol solution of lipid with water (no NaCl) and dialyzed to remove ethanol. Subsequent micrographs show LNPs prepared as in panel (A) and then mixed with NaCl to achieve (B) a 50 mM concentration, (C) a 100 mM concentration, (D) a 150 mM concentration, and (E) a 200 mM concentration. The enlargement in panel (C) shows two interacting discoid particles. The bar represents 200 nm.

what are the effects of including lipids that are not soluble in a lipid bilayer? And finally, what are the effects of including poly(ethylene glycol) (PEG) lipids to inhibit fusion subsequent to vesicle formation?

We show that, for lipid mixtures such as distearoylphosphatidylcholine–cholesterol (DSPC/Chol) mixtures (1:1, mol/mol), the structures produced by ethanol dilution/rapid mixing are small, limit-size bilayer vesicles, as expected. However, considerable morphological diversity is observed if these vesicles experience osmotic stress or if small amounts of cone-shaped lipids such as dioleoylphosphatidylcholine (DOPE) are present. High salt levels induce the formation of bilamellar structures, whereas inclusion of as little as 2 mol % of cone-shaped DOPE results in multilamellar structures that reflect multiple fusion events following the initial

formation of small unilamellar vesicles. The progressive inclusion of triolein (TO), a lipid that is insoluble in a bilayer environment, results in a gradual progression from a bilayer structure to a micellar-like structure containing a hydrophobic inner core. Finally, fusion events can be inhibited by incorporation of small amounts of PEG lipids. This morphological richness offers considerable opportunity for manipulating LNP systems, their contents, and their delivery potential.

## EXPERIMENTAL SECTION

**Materials.** The lipids 1,2-distearoyl-*sn*-glycero-3-phosphocholine (DSPC), 1-palmitoyl-2-oleoyl-*sn*-glycero-3-phospho-(1'-*rac*-glycerol) (POPG), 1,2-dioleoyl-*sn*-glycero-3-phosphoethanolamine (DOPE), 1-palmitoyl-2-hydroxy-*sn*-glycero-3-phosphocholine (16:0 Lyso PC),

1,2-dioleoyl-*sn*-glycero-3-phosphoethanolamine, 1,2-dimyristoyl-rac-glycero-3-methoxypoly(ethylene glycol)-2000 (PEG-DMG), *N*-(7-nitro-2,1,3-benzoxadiazol-4-yl)-1,2-dioleoyl-*sn*-phosphatidylethanolamine (NBD-PE), and *N*-(lissamine rhodamine B sulfonyl)-1,2-dioleoyl-*sn*-phosphatidylethanolamine (Rh-PE) were purchased from Avanti Polar Lipids (Alabaster, AL). Cholesterol (Chol), triolein (TO), and doxorubicin hydrochloride were obtained from Sigma-Aldrich Canada Ltd. (Oakville, Ontario, Canada). Phosphate-buffered saline (PBS) was from GIBCO (Carlsbad, CA). Dialysis membranes (molecular weight cutoff 12,000–14,000 Da) were from Spectrum Laboratories, (Rancho Dominguez, CA). Amicon Ultracel centrifugal units (10 kDa MWCO) were from Millipore (Billerica, MA). The Cholesterol E Total Cholesterol assay kit was provided by Wako Diagnostics (Richmond, VA).

**Preparation of LNPs.** LNPs were prepared by employing a T-tube mixer as previously described.<sup>15</sup> Briefly, lipid components at appropriate ratios were dissolved in ethanol to a concentration of 15 mM total lipid. The aqueous phase consisted of either nonbuffered distilled water or PBS (pH 7.4). The two solutions were mixed through a T-junction mixer at a total flow rate of 20 mL/min and a flow rate ratio of 3:1 vol/vol (corresponding to 15:5 mL/min aqueous/organic phase). The resulting dispersion was subsequently dialyzed against 1000-fold volume of the same aqueous medium (water or PBS) to remove ethanol. Amicon spin concentrators were used to concentrate the resulting LNP dispersions, if needed. Lipid concentrations were determined by measuring total cholesterol using the enzymatic assay.

**Size Analysis of LNPs.** LNPs were sized by dynamic light scattering (DLS) using a Malvern Zetasizer Nano ZS (Malvern, U.K.) following diluting of the sample aliquot with appropriate medium (distilled water or saline). In addition, LNP size characteristics were obtained from cryo-transmission electron microscopy (cryo-TEM) micrographs (as compared by the length to the scalebar).

**Insertion of Lyso PC into LNP's Lipid Bilayers.** LNPs were prepared in water and dialyzed to remove ethanol as described above. Lyso PC was dispersed in water at 10 mg/mL, an aliquot of this dispersion was added to the LNP sample to give 2, 4, 6, and 10% mol compared to the total lipid content (DSPC/Chol 50/50 mol). The mixture was then incubated for 10 min at room temperature (RT) prior to the addition of NaCl.

**Osmotic Pressure.** In all experiments where osmotic gradients were applied, LNPs were prepared in the absence of solutes (i.e., in distilled water) and subsequently mixed with 1M NaCl solution to result in an osmotic pressure gradient (hyperosmotic stress) that causes the water efflux from the LNP's aqueous interior. More specifically, appropriate aliquots of the NaCl solution was added to LNP samples to give a total of 50, 100, 150, and 200 mM final NaCl concentrations.

**Lipid Mixing Assay.** The extent of bilayer fusion as measured by lipid mixing was monitored by the decrease in fluorescence resonance energy transfer (FRET) resulting from dual fluorescent probe dilution.<sup>16</sup> Unlabeled and labeled DSPC/Chol LNPs (the latter containing 0.5 mol % of both NBD-PE and Rh-PE) were prepared in distilled water as described above. Labeled LNPs were diluted to 40  $\mu$ M lipid in a 3 mL quartz cuvette. Fluorescence was monitored with excitation at 465 nm, emission at 535 nm, and an emission cutoff filter at 530 nm. In the absence of osmotic stress, target (unlabeled) LNPs were added in a labeled-to-unlabeled lipid ratio of 1:5 to give a total lipid concentration of 240  $\mu$ M; fluorescence was then monitored over 5 min. In the case of imposed osmotic stress, the hypertonic conditions were generated by the addition of 1M NaCl solution to aqueous LNP dispersion (1:5 labeled/unlabeled) to give a final NaCl concentration of 200 mM and lipid concentration of 240  $\mu$ M, followed by monitoring of the fluorescence increase.

Each measurement was normalized by subtracting the fluorescence observed in the absence of osmotic stress ( $F_0$ ) and dividing by the fluorescence achieved by infinite probe dilution determined by the addition of 25  $\mu$ L of 100 mM Triton X-100 ( $F_{\max}$ ). The percent change in fluorescence was calculated as

$$\% \frac{\Delta F}{\Delta F_{\max}} = 100 \frac{F - F_0}{F_{\max} - F_0}$$

**Cryo-Transmission Electron Microscopy (Cryo-TEM) Analysis of LNP Morphology.** Cryo-TEM imaging was performed using a FEI Tecnai G20 transmission electron microscope (FEI, Hillsboro, OR) as previously described.<sup>15</sup> Prior to imaging, samples were concentrated to approximately 20 mg/mL total lipid, and 3–5  $\mu$ L aliquot of concentrated dispersion was transferred to a glow-discharged copper grid in a FEI Mark IV Vitrobot. The sample was then plunge-frozen into liquid ethane to generate vitreous ice. Frozen samples were stored in liquid nitrogen until imaged. The transmission electron microscope was operated at 200 kV in low-dose mode, and images were obtained using a bottom-mount FEI high-resolution CCD camera (FEI, Hillsboro, OR) at a nominal under focus of 2–4  $\mu$ m. Sample preparation and image acquisition were performed at the UBC Bioimaging Facility (Vancouver, BC).

## RESULTS AND DISCUSSION

**Osmotic Stress Can Stimulate Fusion between Limit-Size DSPC/Cholesterol Systems to Produce Bilamellar Structures.** The process of forming LNP systems using the bottom up procedure first utilized by Batzri and Korn<sup>11</sup> involves mixing lipids dissolved in ethanol with an aqueous medium. Here, we use the T-tube mixing process described in Methods to generate DSPC/Chol (1:1; mol/mol) systems. As shown in Figure 1A, if the aqueous medium used for the mixing process is distilled water, unilamellar vesicle structures are observed as detected by cryo-TEM. However, if these LNPs were subjected to osmotic stress by addition of 1M NaCl to give final salt concentrations of 50, 100, 150 and 200 mM NaCl, very different behavior is observed.

As shown in Figure 1A, LNPs made in distilled water are small ( $\sim$ 50 nm diameter) unilamellar vesicles. Addition of 50 mM NaCl did not result in noticeable changes in size and morphology (Figure 1B). However, if the NaCl concentration in the external medium was adjusted to 100 mM, dramatic changes were observed. Many LNPs adopt a discoid shape, presumably reflecting the effects of osmotic stress (Figure 1C). Most remarkably, those discoid-shaped “deflated” vesicles preferentially interact with each other, forming binary structures of two particles joined at their regions of high curvature (Figure 1C, inset). These structures can be still seen upon exposure to 150 mM NaCl; however, the majority of the LNP population has been converted to bilamellar structures (Figure 1D). At higher osmotic stress conditions (200 mM NaCl), nearly all of the LNPs exhibit bilamellar morphology (Figure 1E).

It is interesting to note that these morphological changes did not result in significant changes in the particle mean size and polydispersity index (PDI) as evidenced by DLS. For example, the size of LNPs before and after the addition of salt (200 mM) was essentially the same (mean size  $\sim$  50 nm, PDI  $\sim$  0.12).

The transition from a unilamellar to bilamellar structure induced by the addition of high salt concentrations must involve membrane fusion. To show that this is the case, we examined lipid mixing between fluorescently labeled and unlabeled DSPC/Chol LNPs in water and in the presence of 200 mM NaCl using a FRET assay.<sup>17</sup> This assay detects the dilution of fluorescent lipid probes arising from the fusion of labeled and unlabeled vesicles and is insensitive to particle aggregation. No increase of fluorescence was observed in the combined labeled/unlabeled sample prior to the addition of NaCl; however, when the combined sample was subjected to

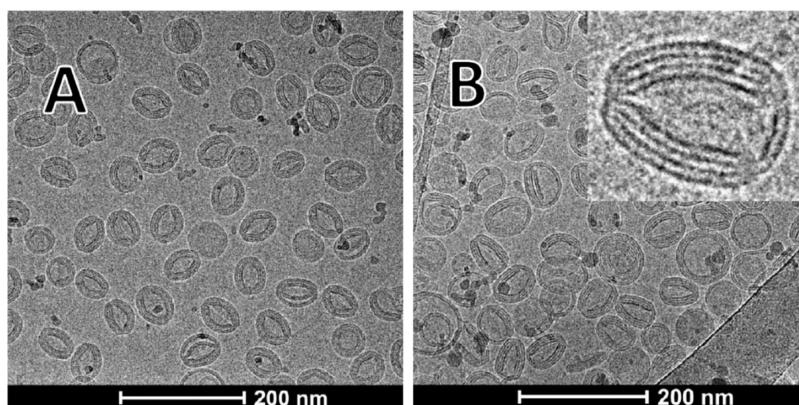


**Figure 2.** Presence of lyso PC can stabilize discoid intermediate structures formed during osmotically induced formation of bilamellar vesicles. DSPC/Chol (50/50) LNPs were prepared as indicated in Methods and dialyzed against distilled water to remove ethanol. Cryo-TEM micrographs were obtained following the addition of 2 mol % lyso PC (panel A) or 10 mol % lyso PC (panel B), followed by the addition of 200 mM NaCl. The inset on panel B shows a blow-up of a representative intermediate structure.

osmotic stress, a rapid increase in fluorescence was detected over the first few seconds, which then plateaued at a maximum of  $\Delta F/\Delta F_{\max} \sim 55\%$  (see Figure S1), demonstrating that the mechanism behind the monolamellar-to-bilamellar transition reflects a membrane fusion process. Note that infinite probe dilution would not be expected as the formation of bilamellar systems corresponds to only one round of fusion.

The mechanism behind the salt-induced transition from a unilamellar to bilamellar structure is of obvious interest. In this regard, the discoid structures observed in Figure 1C appear to be intermediate structures that combine to form bilamellar structures via a fusion event between the regions of high positive curvature at the rim of the disk. To provide supportive evidence that this was the case, it was reasoned that, if the unilamellar-to-bilamellar transition resulted from fusion between regions of high positive curvature, the addition of inverted cone lipids such as lyso PC<sup>18</sup> prior to the addition of NaCl should stabilize the intermediates and inhibit fusion. As shown in Figure 2, this appears to be the case. Addition of as little as 2% mol of lyso PC inhibited fusion on the addition of NaCl and stabilized the intermediate discoid structures (Figure 2A). Addition of more lyso PC (at 4 and 6% mol) resulted in a similar effect (results not shown). When the lyso PC content was increased to 10% mol, it resulted in the formation of a bilayer “bridge” interconnecting the particles (Figure 2B, inset). Note that lyso PC and cholesterol can form bilayer structures, which may account for the observed morphology.<sup>19</sup>

**Increased Negative Curvature Results in the Formation of Multilamellar Systems.** The results of the previous section show that the induction of regions of high positive curvature by osmotic stress can induce fusion between DSPC/chol LNPs and that the addition of inverted cone-shaped lipids to compensate for regions of high positive curvature can inhibit fusion. It may be expected that, if the vesicles experience additional curvature stress, the transitions to bilamellar structures induced by osmotic stress should occur at lower NaCl concentrations. In this regard, higher temperatures increase negative curvature by increasing the area subtended by acyl chains and thus lower NaCl concentrations should be required to induce bilamellar structures. We therefore investigated the morphological behavior of DSPC/Chol systems subjected to osmotic stress at 60 °C. As shown in Figure 3, only 50 mM NaCl is required to induce predominantly bilamellar structures. In addition, the structures

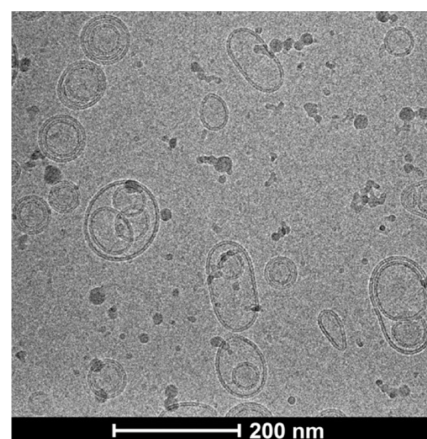


**Figure 3.** Elevated temperatures cause the formation of bilamellar and multilamellar structures at low levels of osmotic stress. The cryo-TEM micrograph was taken of a DSPC/cholesterol (1:1) formulation prepared at 20 °C as for Figure 1 that was then incubated at 60 °C prior to the addition of 50 mM NaCl.

formed were significantly larger ( $\sim 80$  nm) than those produced at room temperature ( $\sim 50$  nm), suggesting that more rounds of fusion took place before the stress induced by the negative curvature of the membrane was relieved to the extent that no further fusion occurred.

**Increased Negative Curvature Results in Fusion of Limit-Size DSPC/Chol LNPs to Form Multilamellar Vesicles.** Having found that promoting negative curvature by increasing temperature results in enhanced fusion of DSPC/Chol vesicles subjected to osmotic stress, it was of obvious interest to find out how the inclusion of cone-shaped lipids that induce negative curvature may affect the morphology of DSPC/Chol LNPs in the absence of osmotic stress. In the first instance, we investigated how the presence of small amounts of DOPE, a cone-shaped lipid that preferentially adopts the hexagonal  $H_{II}$  phase in isolation,<sup>20</sup> can affect the size and morphology of limit-size DSPC/Chol LNPs. DOPE at various amounts (1–4% mol compared to total lipids) was added to equimolar DSPC/Chol dissolved in ethanol, and limit-size systems were produced upon mixing with a distilled water stream as described in Methods. As shown in Figure 4A, systems composed of DSPC/Chol/DOPE (49.5/49.5/1) are similar to those made in the absence of DOPE (see Figure 1A),

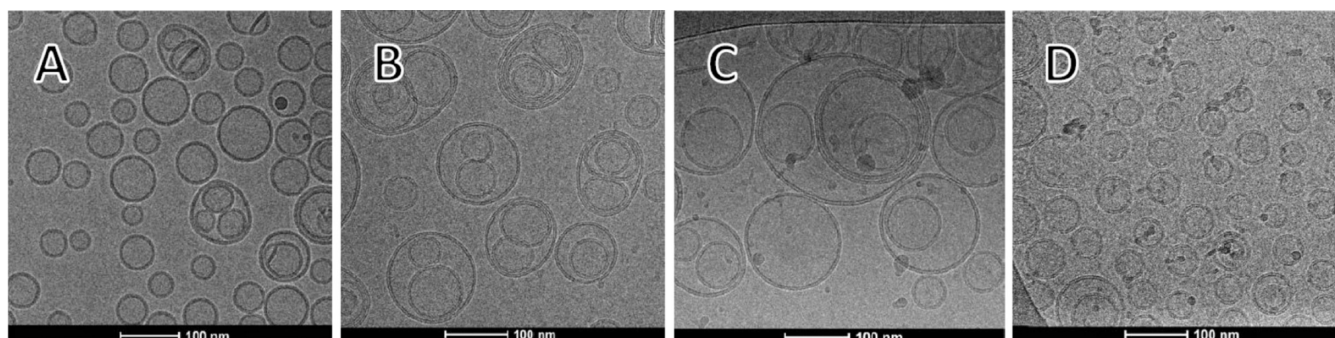


**Figure 4.** Presence of low levels of “cone-shaped” DOPE in DSPC/cholesterol (1:1) mixtures induce the formation of multilamellar structures in distilled water in the absence of osmotic stress. The micrographs show cryo-TEM images of (A) vesicles formed from DSPC/Chol/DOPE (49.5/49.5/1), (B) DSPC/Chol/DOPE (49/49/2), and (C) DSPC/Chol/DOPE (48/48/4) mixtures following ethanol removal. To demonstrate that the structures observed reflect the fusion of limit-size vesicles, the properties of vesicles formed from DSPC/Chol/DOPE/POPG (47.5/47.5/4/1) mixtures were examined. The presence of a negative charge on the vesicles would be expected to inhibit fusion. As noted in panel (D), small unilamellar systems are observed.

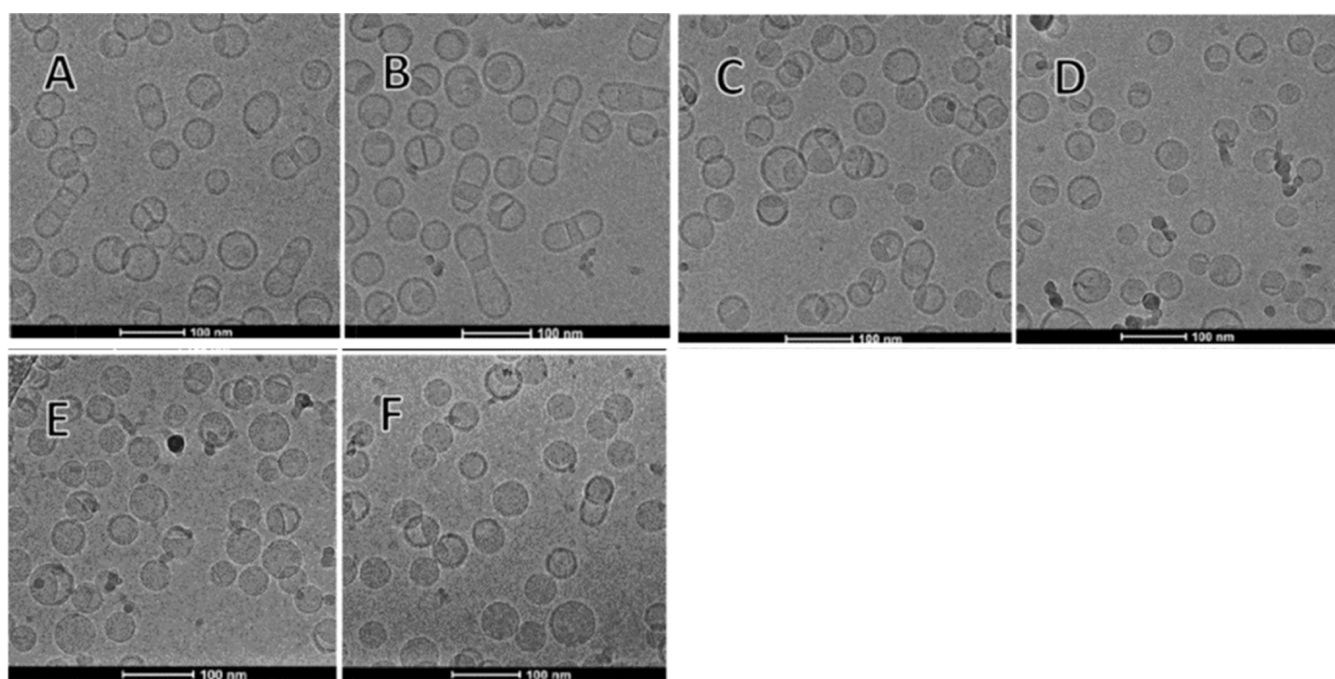


**Figure 5.** Presence of triolein (TO) in DSPC/Chol (1:1) formulations results in progressive formation of “solid core” structure. Lipids in ethanol were formulated using the T-tube process described in Methods, followed by dialysis against distilled water to remove ethanol. The cryo-TEM micrographs were obtained from (A) DSPC/Chol/TO (45/45/10), (B) DSPC/Chol/TO (42.5/42.5/15), (C) DSPC/Chol/TO (40/40/20), (D) DSPC/Chol/TO (35/35/30), (E) DSPC/Chol/TO (30/30/40), and (F) DSPC/Chol/TO (25/25/50).

both in terms of size ( $\sim 55$  nm) and morphology. A small proportion of multivesicular structures, not usually observed for DSPC/Chol (50/50) particles, can be detected. A further increase in the proportion of DOPE to 2% mol had dramatic effects, resulting in much larger ( $\sim 100$  nm diameter), predominantly multivesicular structures (Figure 4B). At 4% DOPE, even larger structures with a similar morphology were formed (Figure 4C). These results clearly indicate that a stable, homogeneous population of monolamellar limit-size LNPs for predominantly DSPC/cholesterol systems cannot be achieved in the presence of as little as 2 mol % DOPE.

It is likely that the multilamellar systems observed in Figure 4B result from the fusion of small unilamellar limit-size vesicles initially produced during the mixing process that fuse to the point where the systems are large enough so that the negative curvature that is driving fusion is relieved. To provide

supportive evidence that this is the case, a small amount of 1-palmitoyl-2-oleoyl-phosphatidylglycerol (POPG) was added to the lipid solution in ethanol prior to mixing with water. The presence of a small amount of the negatively charged POPG would not be expected to change the net curvature of the lipid bilayers as it is a bilayer-forming lipid,<sup>21</sup> however, the presence of a negative charge on the vesicles would be expected to inhibit the close association required for fusion. As shown in Figure 4D, the presence of as little as 1 mol % POPG is sufficient to prevent the formation of multilamellar vesicles for DSPC/Chol/DOPE/POPG (47.5/47.5/4/1) systems, with a mean size of the resulting particles of  $\sim 57$  nm. This size is similar to that of DSPC/Chol (50/50) systems and supports the contention that the multilamellar systems of Figure 5B result from the fusion of unilamellar limit-size vesicles.

**Presence of Lipids Insoluble in a Lipid Bilayer Results in a Progressive Increase in Solid Core Structure.** The studies detailed to this point characterize the influence of factors that change the intrinsic curvature of lipid bilayers on the morphology of LNPs produced by the bottom up rapid mixing/ethanol dilution process. It is of interest to extend these investigations to include lipids such as triolein that are relatively insoluble in lipid bilayers.<sup>22</sup> In contrast to top down procedures such as sonication and extrusion, nonpolar lipids such as triolein that are soluble in ethanol can be readily incorporated into LNP systems using the ethanol dilution/rapid mixing protocol. Previous studies have shown that, for mixtures of 1-palmitoyl-2-oleoyl-phosphatidylcholine (POPC) and high levels of triolein, micellar-like structures can be generated consisting of a monolayer of POPC surrounding a hydrophobic triolein core.<sup>5</sup> However, the morphology of systems containing lower levels of triolein has not been characterized.

The properties of LNPs containing DSPC and cholesterol (DSPC/Chol ratio 1:1; mol/mol) and a range of triolein contents generated using the T-tube mixer were characterized by cryo-TEM (Figure 5) and DLS (Figure 6). As shown in

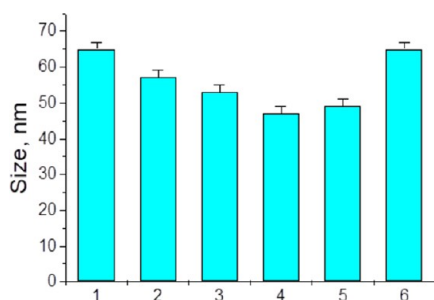


**Figure 6.** Size of DSPC/Chol/TO systems is relatively independent of the TO content. The mean sizes as detected by light scattering were measured for lipid dispersions prepared as for figure and consisting of (1) DSPC/Chol/TO (45/45/10), (2) DSPC/Chol/TO (42.5/42.5/15), (3) DSPC/Chol/TO (40/40/20), (4) DSPC/Chol/TO (35/35/30), (5) DSPC/Chol/TO (30/30/40), and (6) DSPC/Chol/TO (25/25/50).

Figure 5, increasing the proportion of triolein from 10 to 50 mol % leads to the formation of the particles ranging from vesicles with a solid core “bulge” into the aqueous compartment at 10 mol % triolein to solid core systems that presumably correspond to micelles where the triolein core is stabilized by a monolayer of DSPC/Chol. To determine whether this interpretation could be correct, we calculated the proportion of the LNP assuming a constant diameter of 50 nm, a DSPC–cholesterol area per complex of 0.85 nm<sup>2</sup>, and a triolein density of 0.9 mg/mL. As shown in Table 1, the theoretical predictions are in reasonable agreement with observation, where the proportion of the solid core is estimated from the ratio of the solid core area to total area of the LNP depicted in Figure 5.

The theoretical predictions are based on a constant LNP diameter of 50 nm, an area per molecule of DSPC/Chol of 0.85 nm<sup>2</sup>, a triolein density of 0.9 mg/mL, and a membrane thickness of 5 nm. The calculated proportion of the solid core is the ratio of the cross-sectional area of the solid core sphere surrounded by a monolayer of DSPC/Chol to the entire cross-sectional area of the LNP.

**Table 1.** Proportion of LNP That Are Solid Core as Predicted Theoretically and as Measured from the Micrographs Presented in Figure 6

triolein (mol %)	proportion solid core (theory)	proportion solid core (measured), means $\pm$ SD
10	20	20.7 $\pm$ 10.3
15	25	24.3 $\pm$ 11.9
20	30	31.05 $\pm$ 12.3
30	41	46.4 $\pm$ 27.4
40	53	57.3 $\pm$ 25.7
50	67	74.9 $\pm$ 24.5

To further investigate the range of morphologies possible for more complicated systems, we investigated the morphology of Triolein/DSPC/Chol/DOPE LNPs containing 15 mol % triolein and increasing amounts of DOPE. As shown in Figure 7, as little as 2 mol % DOPE results in morphological changes where the solid core is not as intimately attached to the surrounding bilayer, resulting in greater proportions of amoeba-like shapes where a central solid core is surrounded by a lipid bilayer. This trend is increased at 4 mol % DOPE (Figure 7B); in addition, the LNPs are significantly larger. Some of these shapes can be interpreted as LNPs containing a solid core fusing end-to-end to form a tube with a solid core structure in the middle. At 8 mol % DOPE, these putative end-to-end fusion events are taken to an extreme, resulting in large, sunburst structures with bilayer protrusions emanating from a central solid core.

**Low Levels of PEG Lipids Inhibit Fusion during the Ethanol Dialysis Step.** In a final set of experiments, we examined the effect of low levels of PEG lipids on the morphology of the structures observed for different lipid compositions. It would be expected that the presence of PEG lipids, even at low levels, would inhibit fusion events induced by the introduction of lipids such as DOPE that enhance negative curvature and thus promote fusion to relieve membrane stress. To show that this is the case, we investigated the influence of 1 mol % PEG-DMG on the morphology of DSPC/Chol in the absence and presence of 200 mM NaCl, the morphology of DSPC/Chol systems containing 4 mol % DOPE, the morphology of DSPC/Chol systems containing 15 mol % triolein, and finally DSPC/Chol systems containing 4 mol % DOPE and 15 mol % triolein.

As shown in Figure 8A, DSPC/Chol/PEG-DMG (49.5/49.5/1) systems formulated in water were similar in size and morphology to the non-PEGylated DSPC/Chol formulation (see Figure 1A). Although the presence of 1 mol % PEG-DMG did not prevent those systems from transforming to bilamellar vesicles upon the addition of 200 mM NaCl (Figure 8B), the presence of a small proportion of discoid particles is noted. Such structures were not observed in the absence of PEG-DMG (see Figure 1E) and could be accounted for by the stabilization of deflated discoid structures by the adsorption of PEG-DMG in regions of high positive curvature. More dramatically, the presence of 1 mol % PEG-DMG (see Figure 8C) completely prevented the formation of large multivesicular species for DOPE-containing formulations in the absence of osmotic stress (compare with Figure 4C). Further, while the presence of 1 mol % PEG-DMG in DSPC/Chol systems containing 15 mol % TO did not affect the morphology (compare Figure 8D with Figure 5B) in the absence of DOPE, the presence of 1 mol % PEG-DMG inhibited the fusion of

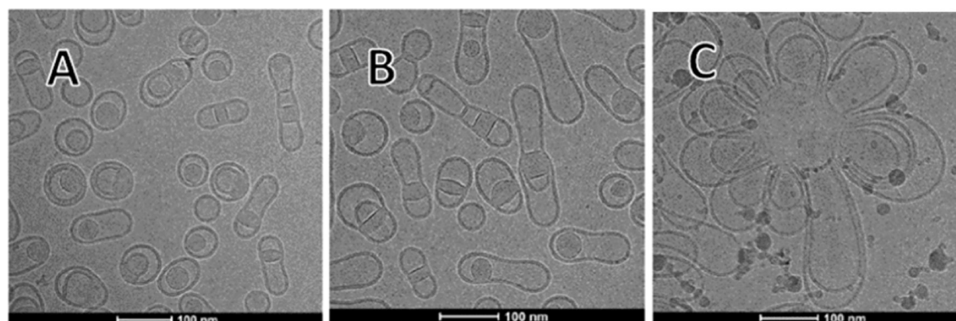


**Figure 7.** Presence of cone-shaped DOPE in TO/DSPC/Chol systems results in progressively larger multilamellar structures. Lipid dispersions were prepared from ethanol solutions containing 15 mol % TO and equimolar levels of DSPC/Chol where DOPE was added at the expense of DSPC/Chol. The cryo-TEM micrographs were obtained for (A) TO/DSPC/Chol/DOPE (15/41.5/41.5/2) dispersions, (B) TO/DSPC/Chol/DOPE (15/40.5/40.5/4) dispersions, and (C) TO/DSPC/Chol/DOPE (15/38.5/38.5/8) dispersions.

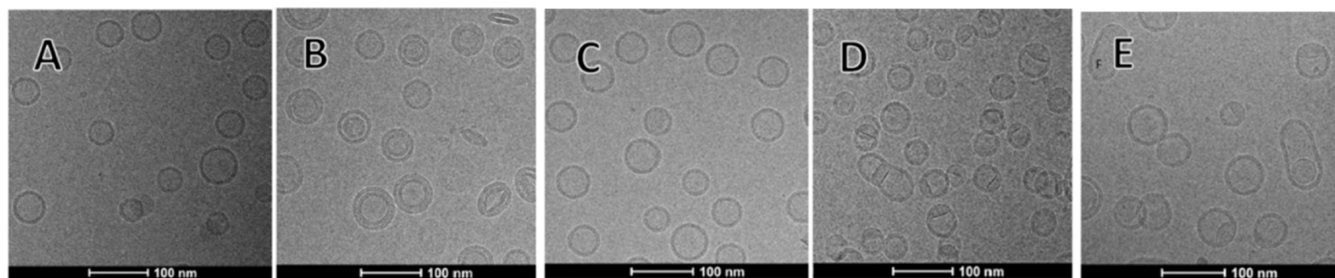


**Figure 8.** Presence of 1 mol % PEG-DMG reduces or inhibits fusion events following the formation of limit-size vesicles. Cryo-TEM micrographs were obtained for lipid dispersions obtained following T-tube mixing with distilled water and subsequent removal of residual ethanol by dialysis. These dispersions were prepared from ethanol lipid solutions consisting of (A) DSPC/Chol/PEG-DMG (49.5/49.5/1), (B) DSPC/Chol/PEG-DMG (49.5/49.5/1) following the addition of 200 mM NaCl, (C) DSPC/Chol/DOPE/PEG-DMG (47.5/47.5/4/1), (D) TO/DSPC/Chol/PEG-DMG (15/42/42/1), and (E) TO/DSPC/Chol/DOPE/PEG-DMG (15/40/40/4/1) dispersions.

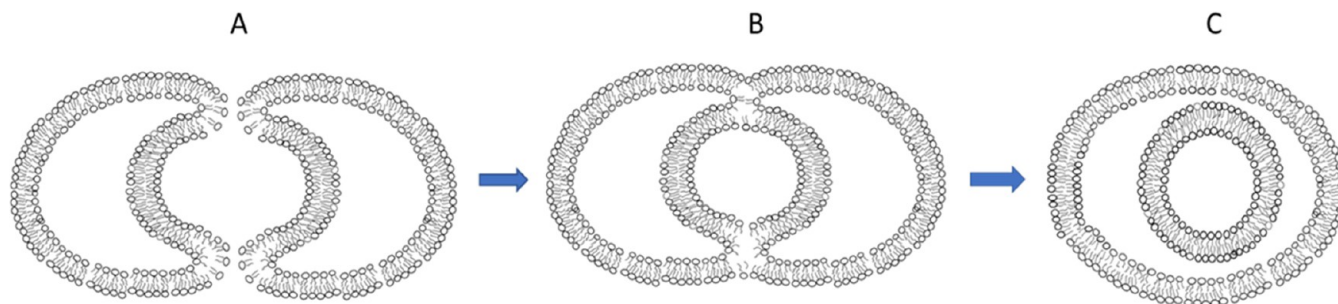


**Figure 9.** The bending stress at the highly curved edges of the “bowl” shaped vesicles produced by osmotic stress (B) is relieved by fusion to produce bilamellar vesicles with a diameter similar to that of parent vesicles (C). Note that, according to this model, only the inner vesicle in the bilamellar systems would be expected to contain the hypertonic medium driving the osmotic stress.

similar systems containing 4 mol % DOPE (compare Figure 8E with Figure 7B).

The results presented here offer insights into how different lipid structures can be engineered by variations in external factors such as osmotic strength or by the judicious adjustment of proportions of component lipids and their relative solubility in one another. There are three topics that warrant further discussion. First, the remarkable transition from a unilamellar to bilamellar structure in the presence of osmotic stress explains previous observations of a bilamellar structure in previous studies, including lipid formulations that are used clinically. Second, the influence of small amounts of inverted cone- or cone-shaped lipids on the morphology of the vesicles offers interesting insight into ways to manipulate the vesicle structure. Finally, the behavior systems containing triolein offer the ability to produce lipid structures with polar and nonpolar

interior compartments. Such systems may have utility as multifunctional drug delivery vehicles. We discuss these topics in turn.

The observation that osmotic stress can cause transitions from a unilamellar to bilamellar structure for vesicles with lipid compositions with robust permeability barrier properties such as DSPC/Chol (1:1) explains previous observations of predominantly bilamellar vesicle structures in a variety of liposomal formulations including the FDA-approved nanomedicine Vyxeos.<sup>23,24</sup> The data presented support a mechanism whereby the osmotic stress produces deflated discoid structures that then anneal at the points of maximum membrane curvature as depicted in Figure 9. This mechanism would predict that only the innermost aqueous compartment of the bilamellar vesicles will contain solutes such as ammonium sulfate (AS) used to form the pH gradients that

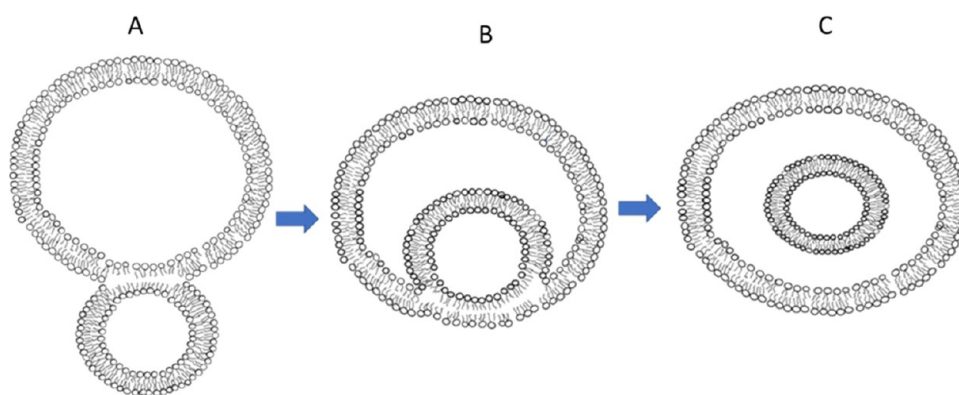


**Figure 10.** Model of the mechanism whereby multilamellar vesicles could form as a result of hemifusion between smaller vesicles and larger ones (A), resulting in an imbalance in surface areas between the inner and outer monolayers and driving an elongated morphology. To return to a spherical morphology, which has the lowest bending energy, this area imbalance could be compensated for by invagination (B), possibly resulting in pinching off of an internalized vesicle, resulting in multilamellar structures (C).

drive the uptake of weak base drugs such as doxorubicin. However, drug uptake will likely be distributed to all compartments as the outer compartment(s) will rapidly become acidified due to efflux of protons from inner compartments to set up and maintain the equilibrium membrane potential.

The behavior of systems containing low levels of cone-shaped DOPE can be interpreted as involving two steps, the initial formation of limit-size unilamellar vesicle systems during the ethanol/water mixing step and then subsequent fusion to form more complicated structures to relieve curvature stress as the ethanol content is reduced from 25% ethanol to zero. This interpretation is supported by the fact that the presence of 1% PEG lipid for systems containing small amounts of DOPE results in unilamellar systems as evidenced by cryo-TEM morphology (Figure 8C,E). In the absence of PEG lipids, it is clear that the presence of DOPE can result in very complicated morphology as demonstrated in Figures 4 and 7. Two features are of interest. First, in the absence of triolein (Figure 4), DOPE induces progressively multilamellar structures. Osmotic forces such as depicted in Figure 9 would not appear to be operating as conditions of low ionic strength are maintained. One possible explanation is that area imbalances between inner and outer monolayers of the larger vesicles formed drive the invagination and formation of internal structures. Specifically, if the presence of DOPE drives hemifusion between smaller vesicles and larger vesicles, the area of the outer monolayer of the larger combined vesicles will be increased more than the area of the inner monolayer, making the vesicle as a whole incompatible with spherical morphology. One way to compensate for this would be for the smaller vesicle to internalize to increase the area of the inner monolayer as shown in Figure 10B. Such structures are also predicted by lowest bending energy considerations.<sup>25</sup> This could possibly lead to complete “pinching off” of internalized vesicles as indicated in Figure 10C.

The presence of DOPE in systems containing 15 mol % triolein (Figure 7) results in different behaviors. In particular, it appears that the presence of DOPE encourages the fusion of vesicles between the ends that contain triolein, resulting in elongated systems with a solid core triolein compartment in the middle. When taken to an extreme at 8 mol % DOPE, all of the solid core regions appear fused together with bilayer

protrusions erupting from this core in a “sunburst” configuration.

The mechanism whereby hybrid lipid structures are formed by the inclusion of hydrophobic molecules such as triolein that are not soluble in lipid bilayers is of interest. It is likely that the first macromolecular entity to fall out of solution as the polarity of the medium is increased during the rapid mixing step is a triolein nucleating particle that then attracts a monolayer of DSPC/Chol.<sup>5</sup> As the polarity increases further, the subsequent deposition of DSPC/Chol onto these nucleating structures in excess of that needed to form the monolayer results in the formation of bilayer “blebs” emanating from the core structure. At the extreme, the bilayer structures can encapsulate the hydrophobic material. A feature of these hybrid systems that is of interest concerns the presence of two compartments, one hydrophobic and the other aqueous, within the same nanoparticle. Such structures offer the possibility of encapsulating two types of materials in a nanoparticle, namely, macromolecular hydrophobic materials that are soluble in the triolein compartment and weak base drugs that can be trapped in the aqueous compartment. Further, these structures are clearly related to the structures observed for high helper lipid contents for systems containing ionizable cationic lipids. As noted elsewhere, very similar structures to those observed for 15 mol % TO in this investigation are observed for LNP systems containing 20 mol % ionizable cationic lipids together with 40 mol % DSPC and cholesterol.<sup>15</sup> Such structures can be accounted for assuming that the ionizable lipid is in the central solid core surrounded by a monolayer of DSPC/Chol (1:1). As noted in Table 1, the hybrid structures observed here for 15 mol % TO can also be rationalized as due to triolein core lipids surrounded first by a monolayer of DSPC/Chol and then by a DSPC/Chol bilayer.

## CONCLUSIONS

In summary, LNP systems produced using the Batzri and Korn ethanol dilution/rapid mixing procedure can exhibit rich morphologies that are exquisitely sensitive to variables such as osmotic strength or relatively minor changes in lipid composition. An understanding of ways to manipulate these morphologies, all of which use scalable self-assembly processes, enhances delivery applications. For example, systems surrounded by a bilayer of DSPC/Chol would be expected to exhibit extended circulation lifetimes *in vivo*.<sup>26</sup> Alternatively,

systems containing two separate compartments such as the aqueous and triolein compartments described here offer the possibility of efficiently loading macromolecular hydrophobic entities and hydrophilic small molecules in the same LNP.

## ■ ASSOCIATED CONTENT

### SI Supporting Information

The Supporting Information is available free of charge at <https://pubs.acs.org/doi/10.1021/acs.langmuir.2c02794>.

Fluorescence levels measured in the mixed (labeled and unlabeled) dispersion of DSPC/Chol LNPs (PDF)

## ■ AUTHOR INFORMATION

### Corresponding Author

Igor V. Zhigaltsev – Department of Biochemistry and Molecular Biology, University of British Columbia, Vancouver, British Columbia V6T 1Z3, Canada; [orcid.org/0000-0002-8368-545X](https://orcid.org/0000-0002-8368-545X); Email: [igorvj@mail.ubc.ca](mailto:igorvj@mail.ubc.ca)

### Author

Pieter R. Cullis – Department of Biochemistry and Molecular Biology, University of British Columbia, Vancouver, British Columbia V6T 1Z3, Canada; [orcid.org/0000-0001-9586-2508](https://orcid.org/0000-0001-9586-2508)

Complete contact information is available at: <https://pubs.acs.org/doi/10.1021/acs.langmuir.2c02794>

### Notes

The authors declare no competing financial interest.

## ■ ACKNOWLEDGMENTS

This research work was supported by Canadian Institutes for Health Research (CIHR FDN 148469).

## ■ REFERENCES

- (1) Bangham, A. D.; Standish, M. M.; Watkins, J. C. Diffusion of univalent ions across the lamellae of swollen phospholipids. *J. Mol. Biol.* **1965**, *13*, 238–252.
- (2) Cullis, P. R.; de Kruijff, B. Lipid polymorphism and the functional roles of lipids in biological membranes. *Biochim. Biophys. Acta, Biomembr.* **1979**, *559*, 399–420.
- (3) Tardieu, A.; Luzzati, V.; Reman, F. C. Structure and polymorphism of the hydrocarbon chains of lipids: a study of lecithin-water phases. *J. Mol. Biol.* **1973**, *75*, 711–733.
- (4) Szoka, F., Jr.; Papahadjopoulos, D. Comparative properties and methods of preparation of lipid vesicles (liposomes). *Annu. Rev. Biophys. Bioeng.* **1980**, *9*, 467–508.
- (5) Zhigaltsev, I. V.; Belliveau, N.; Hafez, I.; et al. Bottom-up design and synthesis of limit size lipid nanoparticle systems with aqueous and triglyceride cores using millisecond microfluidic mixing. *Langmuir* **2012**, *28*, 3633–3640.
- (6) Mayer, L.; Bally, M.; Cullis, P. Uptake of adriamycin into large unilamellar vesicles in response to a pH gradient. *Biochim. Biophys. Acta, Biomembr.* **1986**, *857*, 123–126.
- (7) Haran, G.; Cohen, R.; Bar, L. K.; Barenholz, Y. Transmembrane ammonium sulfate gradients in liposomes produce efficient and stable entrapment of amphipathic weak bases. *Biochim. Biophys. Acta, Biomembr.* **1993**, *1151*, 201–215.
- (8) Felgner, J. H.; Kumar, R.; Sridhar, C.; et al. Enhanced gene delivery and mechanism studies with a novel series of cationic lipid formulations. *J. Biol. Chem.* **1994**, *269*, 2550–2561.
- (9) Semple, S. C.; Klimuk, S.; Harasym, T.; et al. Efficient Encapsulation of Antisense Oligonucleotides in Lipid Vesicles Using Ionizable Aminolipids: Formation of Novel Small Multilamellar Systems. *Biochim. Biophys. Acta, Biomembr.* **2001**, *1510*, 152–166.
- (10) Akinc, A.; Maier, M. A.; Manoharan, M.; et al. The Onpatro story and the clinical translation of nanomedicines containing nucleic acid-based drugs. *Nat. Nanotechnol.* **2019**, *14*, 1084–1087.
- (11) Batzri, S.; Korn, E. D. Single bilayer liposomes prepared without sonication. *Biochim. Biophys. Acta, Biomembr.* **1973**, *298*, 1015–1019.
- (12) Sheetz, M. P.; Chan, S. I. Effect of sonication on the structure of lecithin bilayers. *Biochemistry* **1972**, *11*, 4573–4581.
- (13) Semple, S. C.; Klimuk, S. K.; Harasym, T. O.; et al. Efficient encapsulation of antisense oligonucleotides in lipid vesicles using ionizable aminolipids: formation of novel small multilamellar vesicle structures. *Biochim. Biophys. Acta, Biomembr.* **2001**, *1510*, 152–166.
- (14) Belliveau, N. M.; Huft, J.; Lin, P. J.; et al. Microfluidic Synthesis of Highly Potent Limit-size Lipid Nanoparticles for In Vivo Delivery of siRNA. *Mol. Ther.–Nucleic Acids* **2012**, *1*, No. e37.
- (15) Kulkarni, J. A.; Witzigmann, D.; Leung, J.; Tam, Y. Y. C.; Cullis, P. R. On the role of helper lipids in lipid nanoparticle formulations of siRNA. *Nanoscale* **2019**, *11*, 21733–21739.
- (16) Struck, D. K.; Hoekstra, D.; Pagano, R. E. Use of resonance energy transfer to monitor membrane fusion. *Biochemistry* **1981**, *20*, 4093–4099.
- (17) Hafez, I. M.; Ansell, S.; Cullis, P. R. Tunable pH-sensitive liposomes composed of mixtures of cationic and anionic lipids. *Bioophys. J.* **2000**, *79*, 1438–1446.
- (18) Wu, H.; Zheng, L.; Lentz, B. R. A slight asymmetry in the transbilayer distribution of lysophosphatidylcholine alters the surface properties and poly(ethylene glycol)-mediated fusion of dipalmitoylphosphatidylcholine large unilamellar vesicles. *Biochemistry* **1996**, *35*, 12602–12611.
- (19) Kumar, V. V. Complementary molecular shapes and additivity of the packing parameter of lipids. *Proc. Natl. Acad. Sci. U.S.A.* **1991**, *88*, 444–448.
- (20) Cullis, P.; De Kruijff, B. The polymorphic phase behaviour of phosphatidylethanolamines of natural and synthetic origin. A 31P NMR study. *Biochim. Biophys. Acta, Biomembr.* **1978**, *513*, 31–42.
- (21) Tilcock, C. P. S.; Cullis, P. R. Lipid polymorphism. *Ann. N. Y. Acad. Sci.* **1987**, *492*, 88–102.
- (22) Spooner, P. J. R.; Small, D. M. Effect of free cholesterol on incorporation of triolein in phospholipid bilayers. *Biochemistry* **1987**, *26*, 5820–5825.
- (23) Mayer, L. D.; Tardi, P.; Louie, A. C. CPX-351: a nanoscale liposomal co-formulation of daunorubicin and cytarabine with unique biodistribution and tumor cell uptake properties. *Int. J. Nanomed.* **2019**, *14*, 3819–3830.
- (24) Jeffs, L. B.; Palmer, L. R.; Ambegia, E. G.; et al. A scalable, extrusion-free method for efficient liposomal encapsulation of plasmid DNA. *Pharm. Res.* **2005**, *22*, 362–372.
- (25) Svetina, S.; Zeks, B. Shape behavior of lipid vesicles as the basis of some cellular processes. *Anat. Rec.* **2002**, *268*, 215–225.
- (26) Cullis, P. R.; Mayer, L. D.; Bally, M. B.; Madden, T. D.; Hope, M. J. Generating and loading of liposomal systems for drug-delivery applications. *Adv. Drug Delivery Rev.* **1989**, *3*, 267–282.